Vibrational Spectroscopy 115 (2021) 103272

Contents lists available at ScienceDirect

Vibrational Spectroscopy

journal homepage: www.elsevier.com/locate/vibspec

The pressure-induced structural phase transition of fluorene studied by Raman spectroscopy

A.G.V. Terzidou, N. Sorogas, F. Pinakidou, E.C. Paloura, J. Arvanitidis *

Physics Department, Aristotle University of Thessaloniki, 54124 Thessaloniki, Greece

ARTICLE INFO

Keywords:
Polycyclic aromatic hydrocarbons (PAHs)
Fluorene
Raman spectroscopy
High pressure

ABSTRACT

Raman spectroscopy is used to study the pressure response of crystalline fluorene up to 9 GPa. Pressures higher than 2.5 GPa cause a reversible rearrangement of the molecular stacking, changes in the electronic properties and structural stiffening, leading to a decrease of the pressure coefficients of the intermolecular peak frequencies. The coefficients are further reduced above 6 GPa where fluorene is fully transformed to its isostructural high-pressure phase, while the coexistence of the two phases is evident in the downstroke spectra. The phase transition has less profound effects on the intramolecular modes with the exception of the C–H vibrations.

1. Introduction

Polycyclic aromatic hydrocarbons (PAHs) comprise a large family of molecular systems of two or more fused aromatic rings that have attracted significant attention due to their remarkable physical and chemical properties, stemming from the delocalization of the π-electrons in their aromatic rings. These properties depend on the number of rings comprising the molecules and the dihedral angles between them [1–4]. PAHs and their derivatives find a wide range of applications, including pharmaceuticals, plastics, dyes, liquid crystals and opto-electronic devices [5–7]. Fluorene or 9*H*-fluorene, $C_{13}H_{10}$, is classified as a three-membered ring PAH, even though it is composed of two aromatic hexagonal rings connected by a non-aromatic pentagon into a quasi-planar configuration [8–10]. For commercial purposes, it is obtained from coal tar and its derivatives are used for dyes and anti-inflammatory drugs [11,12]. In the solid state, fluorene forms white molecular crystals that exhibit violet fluorescence, from which its name is derived. At ambient conditions, the crystal structure of fluorene is orthorhombic (space group: *Pnma*) with four molecules in the unit cell, forming a layered herringbone structure that is typical for rigid rod-like organic molecules [9].

In organic molecular crystals, owing to the much weaker intermolecular interactions compared to the strong intramolecular bonding, most of their properties are mainly determined from those of the corresponding individual molecules. Nevertheless, the intermolecular interaction strength, determined by the distance of the constituent molecules and their relative orientation, plays a crucial role in the electronic and optical properties of these systems [13–15]. Moreover, the relative weakness of the intermolecular interactions, renders them by far more sensitive than the intramolecular bonding to external stimuli, such as pressure or temperature [16,17]. Consequently, pressure application on an organic molecular crystal, like solid fluorene, causes the substantial reduction of the intermolecular distances, often followed by changes in the relative orientations of the constituent molecules and structural transitions without altering their chemical structure. This allows the systematic tuning of the electronic and optical characteristics of the system under consideration [18]. Indeed, the high-resolution X-ray diffraction (XRD) study by Heimel et al. has revealed that pressure application higher than 3 GPa on fluorene causes its reversible isostructural phase transition, characterized by abrupt changes in the lattice constants due to a molecular rearrangement from the ambient pressure herringbone pattern towards π-stacking [18]. The low- and the high-pressure phase co-exist up to ~5 GPa, where fluorene crystals are completely transformed to the high-pressure phase of smaller compressibility. In addition, their theoretical calculations predict that pressure application induces a gradual redshift of the energy bandgap, while the new molecular packing in the high-pressure phase alters the bandgap from indirect to direct, and the effective hole masses become comparable to those for conventional semiconductors [18].

Here we report on the pressure response of crystalline fluorene and its structural stability, as determined by Raman spectroscopy for pressures up to 9 GPa. Raman spectroscopy, probing both the intermolecular (external, lattice) and the intramolecular (internal) vibrations, is a non-destructive and versatile tool for the study of molecular crystals and

* Corresponding author.
E-mail address: jarvan@physics.auth.gr (J. Arvanitidis).

https://doi.org/10.1016/j.vibspec.2021.103272
Received 26 March 2021; Received in revised form 26 May 2021; Accepted 27 May 2021
Available online 29 May 2021

their evolution under external perturbations, including pressure application [19–21]. The vibrational spectrum of fluorene has been extensively studied in the past, employing polarized and conventional Raman and/or infrared spectroscopic measurements along with lattice and molecular dynamical calculations, allowing the extensive assignment of both the intermolecular and the intramolecular vibrations [22–31]. Moreover, to our knowledge, there are so far two vibrational studies of crystalline fluorene under high pressure, a Raman spectroscopic one, regarding the intermolecular and the intramolecular modes [32], and a theoretical one, focusing on the intermolecular modes [29]. Nonetheless, both these research works were limited to relatively low pressures (up to 3.5 and 3 GPa, respectively) and hence they reported on the pressure evolution of the mode frequencies solely in the low-pressure phase of fluorene. Finally, high pressure Raman studies of the intermediate frequency (1100–1700 cm^{-1}) intramolecular modes of the poly [2,7-(9,9′-bis(2-ethylhexyl)fluorene] (PF2/6 polyfluorene) revealed significant changes in the peak lineshapes and the pressure dependence of the peak frequencies for pressures higher than 4 GPa [33,34]. These changes were associated with the pressure-induced structural and electronic phase transition reported by Heimel et al. [18,34].

2. Material and methods

Raman spectra of fluorene (Nacalai Tesque Inc.) were recorded in the backscattering geometry using a LabRAM HR (HORIBA) spectrometer. For excitation, the 632.8 nm line of a He-Ne laser was focused on the sample by means of a 50× super long working distance (SLWD) objective, while the laser power was kept below 0.4 mW on the focusing spot of ~2 μm in diameter, in order to eliminate any laser-heating effects. By using the 600 g/mm grating and a confocal pinhole of 80 μm, the spectral width of the system was ~3.5 cm^{-1}. Pressure was generated by a Mao-Bell type diamond anvil cell (DAC) using the ruby fluorescence method for pressure calibration [35]. Daphne 7474 oil, being a non-polar medium (hence it is expected to affect to a lesser extent the fluorene molecular crystals and their pressure response compared to polar fluids) that solidifies at 3.7 GPa at room temperature, was used as the pressure transmitting medium (PTM) [36,37].

3. Results and discussion

The Raman spectrum of fluorene can be divided into two main frequency regions. In the low frequency region (<200 cm^{-1}), the intermolecular (lattice) vibrational modes, as well as the molecular skeleton deformation modes, are expected [22,23]. On the other hand, at higher frequencies, the Raman peaks appearing in the spectrum originate from the intramolecular modes, while particularly those located in the frequency region 2800−3200 cm^{-1} are assigned to C–H stretching vibrations [22,23,30]. First, we focus on the low frequency region. Group theory predicts 21 lattice modes for the *Pnma* space group of the crystalline fluorene at the Γ point of the Brillouin zone (k = 0), belonging to the following irreducible representations: $2b_{1u}+2b_{2u}+2b_{3u}+3a_g+3a_u+3b_{1g}+3b_{2g}+3b_{3g}$, of which 12 correspond to torsional and 9 to translational molecular motions. The 12 intermolecular modes with a_g, b_{1g}, b_{2g}, and b_{3g} symmetries are Raman active [22,25,26,38].

Raman spectra of crystalline fluorene in the frequency region 60−280 cm^{-1} recorded at various pressures are illustrated in Fig. 1. Note that the value of ~60 cm^{-1} corresponds to the lower reliable limit of the obtained spectra due to the Edge Filter cut-off in the spectrometer used. At ambient conditions, three Raman peaks are resolved at 66, 91, and 125 cm^{-1}, attributed to intermolecular modes with b_{1g}, a_g, and a_g symmetry, respectively [22,26]. With increasing pressure, all Raman peaks in the low frequency spectral region shift to higher frequencies, as expected due to the volume contraction and the concomitant bond hardening. At the same time, significant relative intensity changes take place with increasing pressure (Fig. 1(a)). Moreover, with increasing pressure, two additional Raman peaks are resolved, which are distinguished from the peaks at 66 and 91 cm^{-1} owing to their different pressure slopes, while two more peaks enter the studied spectral region from lower frequencies due to their pressure induced hardening. The latter peaks, located at frequencies lower than 60 cm^{-1} at ambient conditions, can be attributed to the b_{1g} and b_{3g} intermolecular modes [22,26]. As for the other two additional peaks appearing at elevated pressures, the Raman peak emerging from that at 66 cm^{-1} could be assigned to an intermolecular mode of b_{1g} symmetry, while that separated from the peak at 91 cm^{-1} to an intermolecular mode of b_{2g}

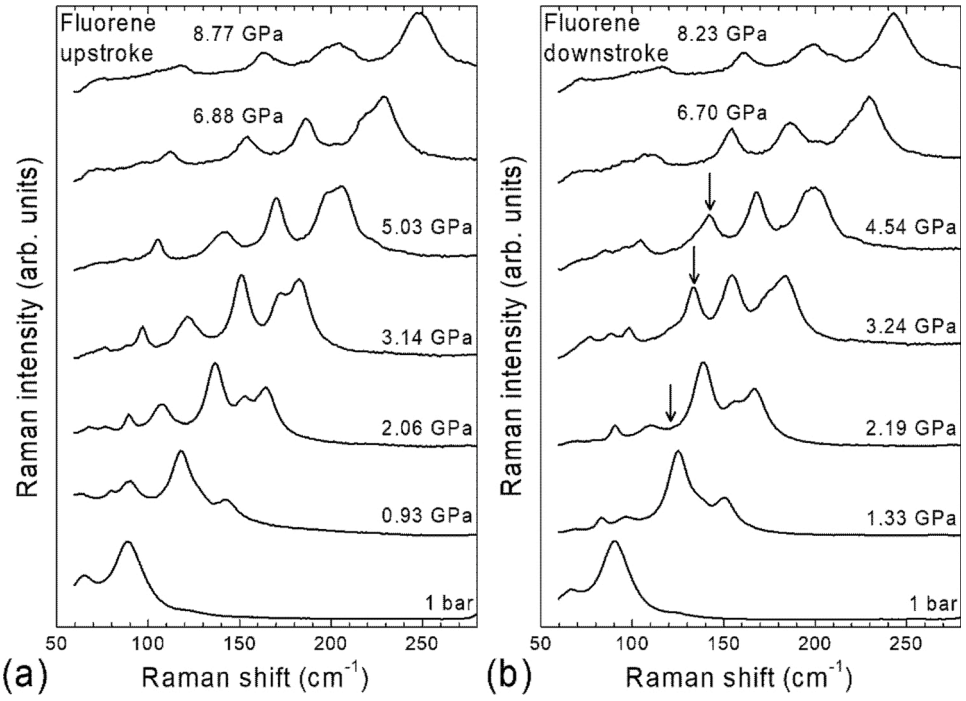

Fig. 1. Raman spectra in the intermolecular (lattice) modes frequency region of fluorene upon pressure (a) increase (upstroke) and (b) decrease (downstroke). Vertical arrow marks a remnant peak of the high-pressure phase upon pressure release that has disappeared in the spectrum recorded at 2.19 GPa.

symmetry [22,26]. However, despite its largest frequency upshift with pressure among all the observed Raman peaks, the detailed polarized high pressure Raman study by Chan et al. has ascribed the second peak to an intramolecular "butterfly" mode of B_1 symmetry, the frequency of which is also expected to be very sensitive to pressure application [32].

The pressure dependence of the frequencies of all the well-resolved Raman peaks in the low frequency region is presented in Fig. 2. For $P <$ 2.5 GPa, the pressure induced frequency shifts of the Raman peaks are quite large and parabolic, as expected for the lattice modes in a molecular crystal where the intermolecular interactions are initially relatively weak and strengthen gradually upon volume contraction [16,17]. Note that similar large frequency shifts for the Raman peaks assigned to the intermolecular modes, compared to the much smaller ones for those corresponding to the intramolecular modes, have also been observed upon cooling of fluorene crystals from 300 K down to 80 K [26]. The coefficients of the linear terms of the quadratic functions used to fit the ω *vs.* *P* data are also given in Fig. 2. These values are in fair agreement with the experimental high pressure Raman study by Chan et al. [32] and the theoretical one by Serov et al. [29]; the only exception is the overestimation of the pressure slope for the a_g mode at 125 cm^{-1} in the theoretical study (almost double as that obtained experimentally here and in Ref. [32]).

For pressures higher than 2.5 GPa, the gradual structural transformation of fluorene to its high-pressure phase, having almost double bulk modulus ($B_0 = 11.3$ GPa) than that of the low-pressure phase ($B_0 = 5.9$ GPa), as well as reduced pressure derivative B'_0 (5.4 from the value of 7.5 at low pressures) [18], cause the quasi-linear pressure evolution of the Raman peak frequencies and the decrease of their pressure coefficients. The pressure coefficients further decrease above 6 GPa, where the studied material is fully transformed to its high-pressure phase associated with the molecular stacking rearrangement (Fig. 2). As can be inferred from Fig. 2, the number of the observed Raman peaks is generally retained in the high-pressure phase, except for the appearance of a rather weak peak at ~200 cm^{-1} above 6 GPa. This experimental observation is compatible with the isostructural nature of the phase transition observed by XRD [18].

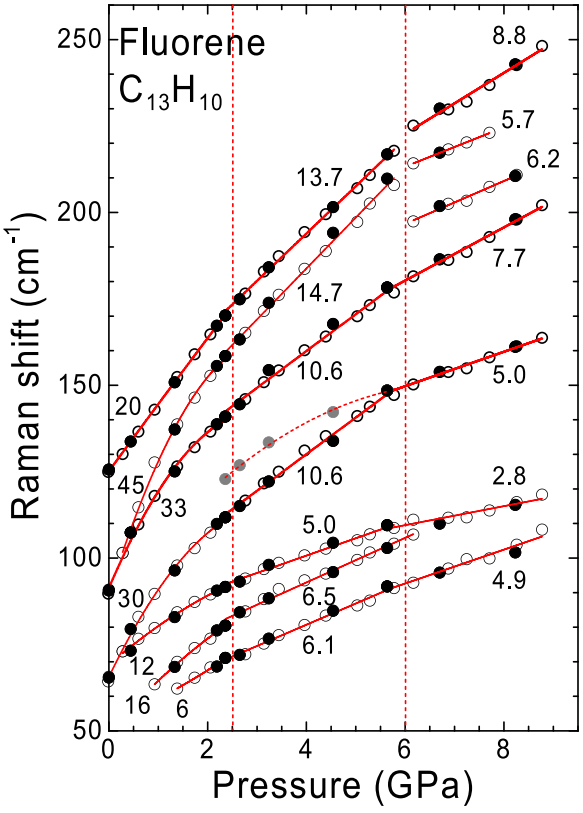

Fig. 2. Frequencies of the intermolecular (lattice) Raman peaks of fluorene as a function of pressure. Open (solid) circles correspond to data obtained upon pressure increase (decrease). Thicker edge thickness symbols indicate stronger Raman peaks upon pressure increase. Grey solid circles correspond to a remnant Raman peak of the high-pressure phase of fluorene upon pressure release. Red lines through the experimental data are their least-square fitting, while numbers refer to the pressure slopes of the corresponding Raman peak frequencies. Dotted vertical lines indicate pressure values where changes in the pressure evolution of the Raman peak frequencies occur.

It is worth pointing out that there is no apparent phase coexistence in the pressure region 3−5 GPa for the Raman spectra recorded upon pressure increase (Fig. 1(a)), as that observed in the case of the high pressure XRD data [18]. Nevertheless, upon pressure decrease, there is clear retention of the stiffer high-pressure phase down to ~2.4 GPa, reflected by the Raman peak marked by the vertical arrows in Fig. 1(b), while the corresponding b_{1g} mode of the low-pressure phase at lower frequencies emerges and gains gradually in intensity at the expense of the former. The pressure dependence of the frequency position of this high-pressure remnant Raman peak is represented in Fig. 2 by the grey solid circles and appears to be parabolic. Note that the solidification pressure (3.7 GPa [36]) of the PTM used is well above the pressure of 2.5 GPa where the changes of the pressure dependence of the Raman peak frequencies begin upon pressure increase. The worse hydrostaticity of the PTM at the highest pressure attained in our experiments (~9 GPa) could influence the pressure evolution of the Raman spectra upon pressure decrease. However, the pressure induced frequency shifts of all the other intermolecular Raman peaks are fully reversible upon pressure decrease (Fig. 2). Moreover, the direct comparison between the Raman spectra illustrated in Fig. 1(b) (downstroke experiment) with those in Fig. 1(a) (upstroke experiment) reveals that, apart from the spectral region including the aforementioned remnant peak, the pressure induced changes of the relative intensities are also reversible. The spectrum of the sample recovered after the complete pressure cycle is apparently the same as that of the starting material (bottom spectra in Fig. 1(a) and (b)).

Raman spectra of crystalline fluorene recorded in the whole spectral region at various pressures (upstroke data) are illustrated in Fig. 3. As can be inferred from the figure, with increasing pressure, almost all the intramolecular modes exhibit a hardening but, as expected, with significantly reduced rates than those for the intermolecular vibrations. Above 3 GPa, the overall enhancement and the strong modification of the -electronic in origin- background lineshape in the frequency region ω < 700 cm^{-1}, possibly signal the onset of the electronic transition predicted theoretically by Heimel et al. to accompany the pressure induced structural transition [18]. As was mentioned in the introductory section, their density functional calculations revealed the decrease of the indirect bandgap of crystalline fluorene, which turns into a direct one (thus implicating an enhanced luminescence signal in the visible spectral region) upon molecular reorientation and stacking rearrangement in the high-pressure phase of the system, caused by the increase of the electronic band widths and curvatures. This electronic transition should also be the cause for the significant intensity redistribution among the Raman peaks and the change of the overall spectrum profile in the intermolecular and C–H stretching vibrations frequency regions at ~3 GPa (Fig. 3).

The majority of the peaks in the Raman spectrum of fluorene in the frequency region >250 cm^{-1} has been assigned to particular intramolecular vibrations [22,23,27,28,30]. Note that for the C_{2v} symmetry of an individual fluorene molecule (in the solid state, the site symmetry is C_s), the vibrational spectrum consists of 22 A_1, 10 A_2, 11 B_1, and 20 B_2 in-plane and out-of-plane vibrational modes, all of them being Raman active, though in several cases with vanishingly small intensities [22,30,39,40]. The pressure dependence of the frequencies of all the well-resolved Raman peaks in the intermediate frequency region (250−1700 cm^{-1}), mainly corresponding to the intramolecular

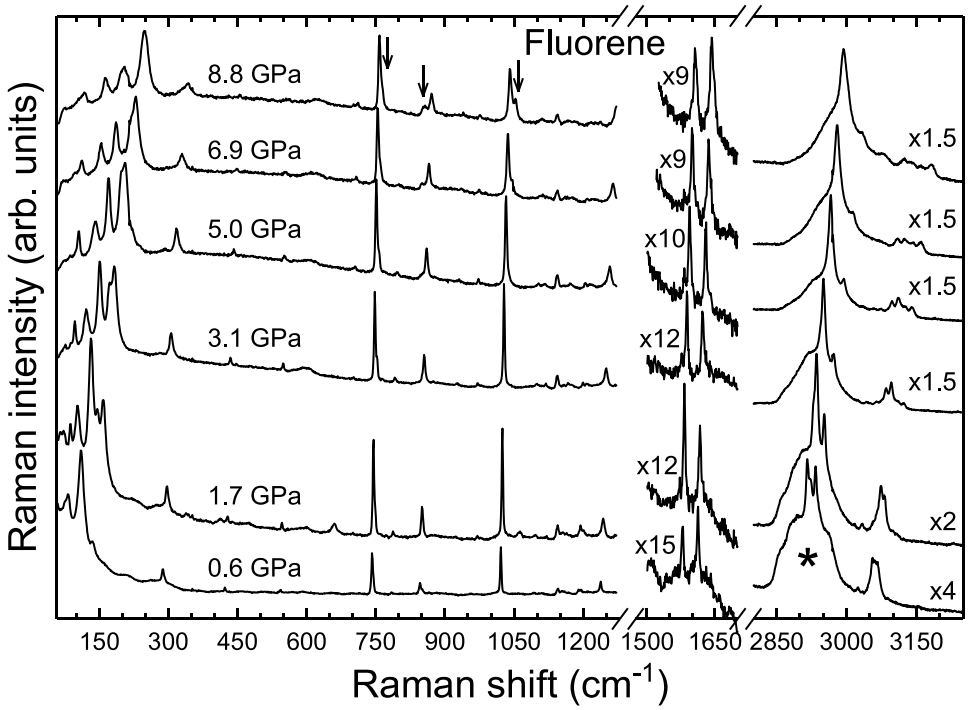

Fig. 3. Raman spectra of fluorene recorded at various pressures. The frequency region 1300–1400 cm^{-1} has been excluded due to the strong Raman signal of the diamond anvils. Arrows denote Raman peaks appearing in the spectra at elevated pressures, while asterisk marks the broad Raman band originating from the C–H stretching vibrations of the Daphne oil used as the PTM.

backbone and aromatic vibrational modes, is presented in Fig. 4(a) and (b) along with their linear pressure coefficients $\partial\omega/\partial P$. All these pressure coefficients are positive, except for the Raman peak at 1146 cm^{-1}, associated with the in-plane C–H bending [23,28], which exhibits a small negative value for $P < 2.5$ GPa. As in the intermolecular modes, the pressure dependencies of the intramolecular peak frequencies are also compatible with the earlier high pressure Raman study in the low-pressure phase of fluorene by Chan et al. [32].

Apart from the Raman peaks at 1576 and 1611 cm^{-1}, attributed to the in-plane quadrant stretching of the hexagonal rings [23,28], the pressure coefficients and/or the pressure evolution of the peak frequencies undergo small changes on going from the low- to the high-pressure phase of crystalline fluorene. Of particular interest is the pressure evolution of the Raman peaks in the frequency region 700−1050 cm^{-1} (Fig. 4(b)) that are mainly assigned to C–H in-plane scissoring or rocking and out-of-plane wagging vibrations [23,28]. Hence, these intramolecular vibrations are expected to be quite sensitive to the changes in the molecular environment caused by the structural transition of fluorene. As the material enters the high-pressure phase, weak satellite Raman peaks (marked by the vertical arrows in Fig. 3)

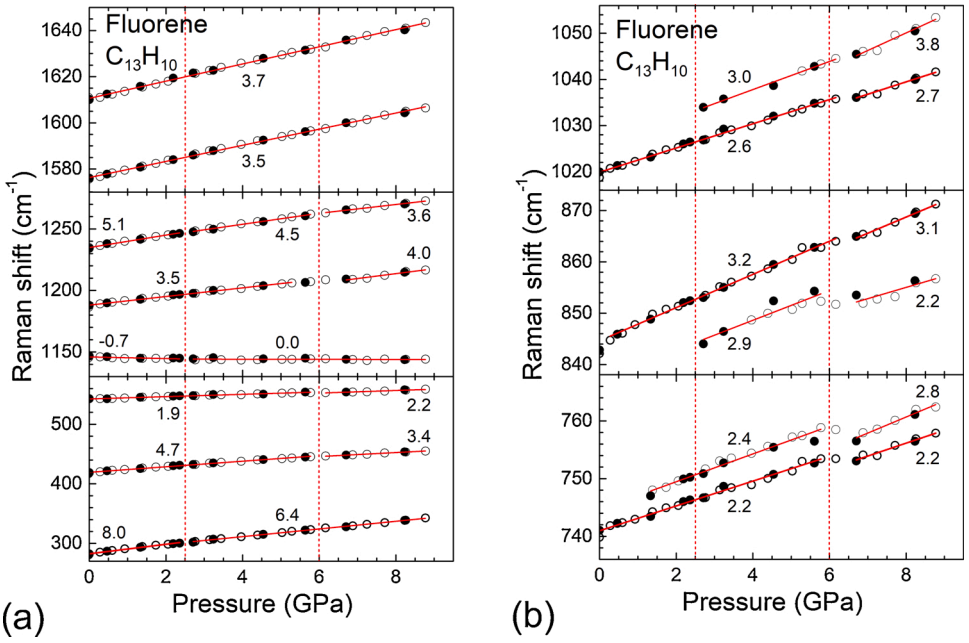

Fig. 4. Frequencies of well-resolved intramolecular (internal) Raman peaks of fluorene at various frequency regions as a function of pressure. Open (solid) circles correspond to data obtained upon pressure increase (decrease). Thicker edge thickness symbols indicate stronger Raman peaks upon pressure increase. Red lines through the experimental data are their least-square fitting, while numbers refer to the pressure slopes of the corresponding Raman peak frequencies. Dotted vertical lines indicate pressure values, where changes in the pressure evolution of the intermolecular Raman peak frequencies occur.

appear close to the stronger pre-existing ones with similar pressure slopes. The appearance of these peaks is a strong indication of differentiations within a fluorene molecule in the C–H environments due to the different molecular orientations and packing in the high-pressure phase. Moreover, all Raman peaks presented in Fig. 4(b) exhibit small frequency redshifts in the pressure region ~6 GPa, being suggestive of a rather abrupt strengthening of the molecule-molecule interactions during the complete transformation of the studied material to its high-pressure phase, causing, in turn, the softening of the intramolecular C–H bending.

The pressure dependence of Raman peak frequencies attributed to the intramolecular C–H stretching vibrations in fluorene is shown in Fig. 5. In agreement with the high pressure Raman study by Chan et al. [32], the frequencies of these vibrations exhibit the larger pressure shifts among the intramolecular modes, befitting the peripheral nature of the hydrogen atoms in the fluorene molecule. The Raman peaks in this frequency region also undergo significant intensity redistribution with increasing pressure, appearing quite sensitive to volume contraction and molecular reorientation. The structural transition of fluorene causes again the reduction of the majority of the pressure coefficients of the peak frequencies (numbers in Fig. 5), with the exception of the two higher frequency C–H stretching vibrations where the pressure coefficients increase in the high-pressure phase. All these spectral changes, regarding the frequency shifts and the relative intensity of the observed peaks, as well as the pressure coefficients of the peak frequencies, are fully reversible upon pressure decrease. Noticeably, according to the data presented in Fig. 5, the frequencies of the quite strong Raman peaks

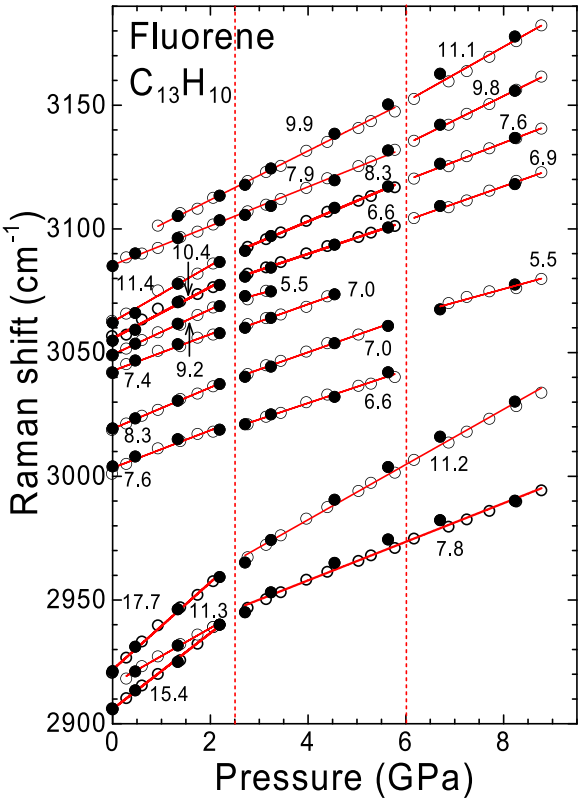

Fig. 5. Pressure dependence of the well-resolved intramolecular Raman peak frequencies originating from the C–H stretching vibrations of fluorene as a function of pressure. Open (solid) circles correspond to data obtained upon pressure increase (decrease). Thicker edge thickness symbols indicate stronger Raman peaks upon pressure increase. Red lines through the experimental data are their least-square fitting, while numbers refer to the pressure slopes of the corresponding Raman peak frequencies. Dotted vertical lines indicate pressure values, where changes in the pressure evolution of the intermolecular Raman peak frequencies occur.

at 2906 and 2916 cm^{-1} (attributed, respectively, to the asymmetric (B_1 symmetry) and the totally symmetric (A_1 symmetry) C–H stretching vibrations in the CH_2 units of the "free" pentagon vertex [22,28]) are more susceptible to pressure application and the structural transition of crystalline fluorene from the herringbone pattern to the π-stacking.

Similar to fluorene, subtle structural transitions at moderate pressure conditions ($P \leq$ 6 GPa) have also been observed by means of vibrational (Raman and/or infrared) spectroscopy in various PAHs with molecules comprised by 2–4 hexagonal carbon rings (naphthalene, biphenyl, anthracene, phenanthrene, and pyrene), including parent benzene [21, 41–43]. These transitions are usually associated with rearrangement of the molecular orientations and stacking without any considerable distortion of the constituent molecules. Moreover, they appear to be kinetically sluggish and reversible, as in the case of fluorene studied here. Therefore, the findings of the present work complete the picture regarding the pressure response of the vibrational modes of the basic PAH materials and the peculiarities induced by molecular reorientation and structural transitions.

4. Conclusion

To conclude, we have presented here a detailed study of the pressure response up to 9 GPa of both the intermolecular and the intramolecular Raman modes of crystalline fluorene. The pressure evolution of the Raman spectra and the frequencies of the Raman peaks authenticate the reversible and sluggish isostructural phase transition of the material in the pressure range 2.5−6 GPa, characterized by the reorientation and the different stacking of the fluorene molecules. Our experimental data at elevated pressures are also compatible with the theoretically predicted changes in the electronic properties of fluorene crystals upon the pressure-induced transformation to their high-pressure phase.

CRediT authorship contribution statement

A.G.V. Terzidou: Participation in experiments, data analysis, Writing - original draft. **N. Sorogas:** Participation in experiments, review & editing. **F. Pinakidou:** Data analysis, review & editing. **E.C. Paloura:** Writing - review & editing, Supervision. **J. Arvanitidis:** Conceptualization, data analysis, Writing - original draft, Supervision.

Declaration of Competing Interest

The authors report no declarations of interest.

Acknowledgements

This research is co-financed by Greece and the European Union (European Social Fund- ESF) through the Operational Programme «Human Resources Development, Education and Lifelong Learning 2014-2020» in the context of the project "Spectroscopic studies of PAHs molecular systems" (MIS 5047932). The authors also acknowledge the Center for Interdisciplinary Research and Innovation of the Aristotle University of Thessaloniki (CIRI-AUTH) for the use of Raman instrumentation.

References

[1] L. Del Freo, A. Painelli, A. Girlando, Z.G. Soos, Electronic defects and conjugation length in mesoscopic π-systems, Synth. Met. 116 (2001) 259–262, https://doi.org/10.1016/S0379-6779(00)00463-X.
[2] H.W. Furumoto, H. Ceccon, Ultraviolet organic liquid lasers, IEEE J. Quant. Electron. 6 (1970) 262–268, https://doi.org/10.1109/JQE.1970.1076451.
[3] P. Garrigues, M. Radke, O. Druez, H. Willsch, J. Bellocq, Reversed-phase liquid chromatographic retention behavior of dimethylphenanthrene isomers, J. Chromatogr. 473 (1989) 207–213, https://doi.org/10.1016/S0021-9673(00)91302-5.
[4] T.K. Ahn, K.S. Kim, D.Y. Kim, S.B. Noh, N. Aratani, C. Ikeda, A. Osuka, D. Kim, Relationship between two-photon absorption and the π-conjugation pathway in

porphyrin arrays through dihedral angle control, J. Am. Chem. Soc. 128 (2006) 1700–1704, https://doi.org/10.1021/ja056773a.
[5] A.H. Neilson (Ed.), PAHs and Related Compounds Chemistry, Springer-Verlag, Berlin Heidelberg GmbH, 1998.
[6] J.E. Anthony, Functionalized acenes and heteroacenes for organic electronics, Chem. Rev. 106 (2006) 5028–5048, https://doi.org/10.1021/cr050966z.
[7] Q. Ye, C. Chi, Recent highlights and perspectives on acene based molecules and materials, Chem. Mater. 26 (2014) 4046–4056, https://doi.org/10.1021/cm501536p.
[8] D.M. Burns, J. Iball, Molecular structure of fluorene, Nature 173 (1954) 635, https://doi.org/10.1038/173635a0.
[9] V.K. Belsky, V.E. Zavodnik, V.M. Vozzhennikov, Fluorene, $C_{13}H_{10}$, Acta Cryst. C 40 (1984) 1210–1211, https://doi.org/10.1107/S0108270184007368.
[10] R.E. Gerkin, A.P. Lundstedt, W.J. Reppart, Structure of fluorene, $C_{13}H_{10}$, at 159 K, Acta Cryst. C 40 (1984) 1892–1894, https://doi.org/10.1107/S0108270184009963.
[11] I.V. Kurdyukova, A.A. Ishchenko, Organic dyes based on fluorene and its derivatives, Rus. Chem. Rev. 81 (2012) 258–290, https://doi.org/10.1070/RC2012v081n03ABEH004211.
[12] A.V. Dean, S.J. Lan, K.J. Kripalani, L.T. Difazio, E.C. Schreiber, Metabolism of the (+)-, (±)-, and (-)-enantiomers of α-methylfluorene-2-acetic acid (cicloprofen) in rats, Xenobiotica 7 (1977) 549–560, https://doi.org/10.3109/00498257709038690.
[13] J.-W. van der Horst, P.A. Bobbert, M.A.J. Michels, G. Brocks, P.J. Kelly, *Ab initio* calculation of the electronic and optical excitations in polythiophene: effects of intra- and interchain screening, Phys. Rev. Lett. 83 (1999) 4413–4416, https://doi.org/10.1103/PhysRevLett.83.4413.
[14] A. Ruini, M.J. Caldas, G. Bussi, E. Molinari, Solid state effects on exciton states and optical properties of PPV, Phys. Rev. Lett. 88 (2002), 206403, https://doi.org/10.1103/PhysRevLett.88.206403.
[15] P. Puschnig, C. Ambrosh-Draxl, Suppression of electron-hole correlations in 3D polymer materials, Phys. Rev. Lett. 89 (2002), 056405, https://doi.org/10.1103/PhysRevLett.89.056405.
[16] R. Zallen, Pressure-Raman effects and vibrational scaling laws in molecular crystals: S_8 and As_2S_3, Phys. Rev. B 9 (1974) 4485–4496, https://doi.org/10.1103/PhysRevB.9.4485.
[17] R. Zallen, M.L. Slade, Influence of pressure and temperature on phonons in molecular chalcogenides: crystalline As_4S_4 and S_4N_4, Phys. Rev. B 18 (1978) 5775–5798, https://doi.org/10.1103/PhysRevB.18.5775.
[18] G. Heimel, K. Hummer, C. Ambrosh-Draxl, W. Chunwachirasiri, M.J. Winokur, M. Hanfland, M. Oehzelt, A. Aichholzer, R. Resel, Phase transition and electronic properties of fluorene: a joint experimental and theoretical high-pressure study, Phys. Rev. B 73 (2006), 024109, https://doi.org/10.1103/PhysRevB.73.024109.
[19] I. Orgzall, F. Emmerling, B. Schulz, O. Franco, High-pressure studies on molecular crystals - relations between structure and high-pressure behavior, J. Phys. Condens. Matter 20 (2008), 295206, https://doi.org/10.1088/0953-8984/20/29/295206.
[20] M. Guerain, A review on high pressure experiments for study of crystallographic behavior and polymorphism of pharmaceutical materials, J. Pharm. Sci. 109 (2020) 2640–2653, https://doi.org/10.1016/j.xphs.2020.05.021.
[21] E. O'Bannon III, Q. Williams, Vibrational spectra of four polycyclic aromatic hydrocarbons under high pressure: implications for stabilities of PAHs during accretion, Phys. Chem. Miner. 43 (2016) 181–208, https://doi.org/10.1007/s00269-015-0786-1.
[22] A. Bree, R. Zwarich, Vibrational assignment of fluorene from the infrared and Raman spectra, J. Chem. Phys. 51 (1969) 912–920, https://doi.org/10.1063/1.1672155.
[23] C. Decker, Laser-Raman spectroscopy of disubstituted spiro-cyclopropane-1,9'-fluorene stereoisomers, Spectrochim. Acta A. 35 (1979) 1303–1306, https://doi.org/10.1016/0584-8539(79)80081-1.
[24] G. Filippini, C.M. Gramaccioli, M. Simonetta, Lattice-dynamical calculations for fluorene, carbazole, dibenzofuran and dibenzothiophen, Chem. Phys. Lett. 79 (1981) 470–475, https://doi.org/10.1016/0009-2614(81)85016-6.
[25] B. Prass, J.P. Colpa, D. Stehlik, Identification of the lowest energy nuclear fluctuation modes promoting the photochemical H-transfer tunneling reaction in doped fluorene single crystals, J. Phys. Chem. 88 (1988) 191–197, https://doi.org/10.1063/1.454635.
[26] B. Prass, J.P. Colpa, D. Stehlik, Intermolecular H-tunneling in a solid state photoreaction promoted by distinct low-energy nuclear fluctuation modes, Chem. Phys. 136 (1989) 187–199, https://doi.org/10.1016/0301-0104(89)80046-1.
[27] L. Cuff, M. Kertesz, Theoretical prediction of the vibrational spectrum of fluorene and planarized poly(p-phenylene), J. Phys. Chem. 98 (1994) 12223–12231, https://doi.org/10.1021/j100098a017.
[28] S.Y. Lee, B.H. Boo, Density functional theory study of vibrational spectra of fluorene, J. Phys. Chem. 100 (1996) 8782–8785, https://doi.org/10.1021/jp960020g.
[29] S.A. Serov, M.V. Bazilevskii, V.A. Tikhomirov, Phonon spectrum of a fluorene molecular crystal, Russ. J. Phys. Chem. A 81 (2007) 291–296, https://doi.org/10.1134/S0036024407020240.
[30] S. Chakraborty, P. Das, S. Manogaran, P.K. Das, Vibrational spectra of fluorene, 1-methylfluorene and 1,8-dimethylfluorene, Vib. Spectrosc. 68 (2013) 162–169, https://doi.org/10.1016/j.vibspec.2013.07.001.
[31] K.H. Michaelian, S.A. Oladepo, J.M. Shaw, X. Liu, D. Bégué, I. Baraille, Raman and photoacoustic infrared spectra of fluorene derivatives: experiment and calculations, Vib. Spectrosc. 74 (2014) 33–46, https://doi.org/10.1016/j.vibspec.2014.07.003.
[32] I.Y. Chan, M.S. Dernis, C.M. Wong, B. Prass, D. Stehlik, High pressure studies of the acridine/fluorene photoreaction: vibration assisted tunneling, J. Chem. Phys. 103 (1995) 2959–2969, https://doi.org/10.1063/1.470483.
[33] C.M. Martin, S. Guha, M. Chandrasekhar, H.R. Chandrasekhar, R. Guentner, P. Scanduicci de Freitas, U. Scherf, Hydrostatic pressure dependence of the luminescence and Raman frequencies in polyfluorene, Phys. Rev. B 68 (2003), 115203, https://doi.org/10.1103/PhysRevB.68.115203.
[34] S. Guha, Raman spectroscopic studies of polyfluorenes, Open J. Phys. Chem. 2 (2008) 6–12, https://doi.org/10.2174/1874067700802010006.
[35] H.K. Mao, J. Xu, P.M. Bell, Calibration of the ruby pressure gauge to 800 kbar under quasi-hydrostatic conditions, J. Geophys. Res. 91 (1986) 4673–4676, https://doi.org/10.1029/JB091iB05p04673.
[36] K. Murata, K. Yokogawa, H. Yoshino, S. Klotz, P. Munsch, A. Irizawa, M. Nishiyama, K. Iizuka, T. Nanba, T. Okada, Y. Shiraga, S. Aoyama, Pressure transmitting medium Daphne 7474 solidifying at 3.7 GPa at room temperature, Rev. Sci. Instrum. 79 (2008), 085101, https://doi.org/10.1063/1.2964117.
[37] S. Sasaki, S. Kato, T. Kume, H. Shimizu, T. Okada, S. Aoyama, F. Kusuyama, K. Murata, Elastic properties of new-pressure transmitting medium Daphne 7474 under high pressure, J. Appl. Phys. 49 (2010), 106702, https://doi.org/10.1143/JJAP.49.106702.
[38] A.I. Kitaigorodsky (Ed.), Molecular Crystals and Molecules, Academic Press Inc., New York, 1973.
[39] D.M. Burns, J. Iball, The crystal and molecular structure of fluorene, Proc. R. Soc. Lond. A 227 (1955) 200–214, https://doi.org/10.1098/rspa.1955.0004.
[40] K. Witt, Vibrational analysis of fluorene, Spectrochim. Acta A 24 (1968) 1115–1123, https://doi.org/10.1016/0584-8539(68)80131-X.
[41] D.M. Adams, R. Appleby, Vibrational spectroscopy at very high pressures. Part 18.-Three solid phases of benzene, J. Chem. Soc. Faraday Trans. 73 (1977) 1896–1905, https://doi.org/10.1039/F29777301896.
[42] M. Zhou, K. Wang, Z. Mena, S. Gao, Z. Li, C. Sun, Study of high-pressure Raman intensity behavior of aromatic hydrocarbons: benzene, biphenyl and naphthalene, Spectrochim. Acta A 97 (2012) 526–531, https://doi.org/10.1016/j.saa.2012.07.001.
[43] K.P. Meletov, Phonon spectrum of a naphthalene crystal at a high pressure: influence of shortened distances on the lattice and intramolecular vibrations, Phys. Solid State 55 (2013) 581–588, https://doi.org/10.1134/S1063783413030207.